



Cite this: DOI: 10.1039/c7cc03823b

Received 17th May 2017,
Accepted 19th June 2017

DOI: 10.1039/c7cc03823b

rsc.li/chemcomm

Platinum(II) photo-catalysis for highly selective difluoroalkylation reactions†

Jian-Ji Zhong,^{ab} Chen Yang,^{cd} Xiao-Yong Chang,^{ac} Chao Zou,^{id ab} Wei Lu^{id a} and
Chi-Ming Che^{*acd}

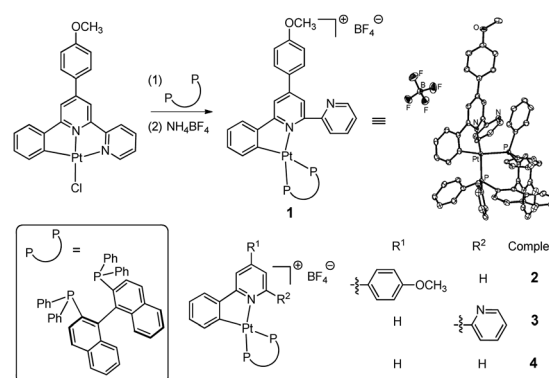
The platinum(II) photo-catalyzed difluoroalkylation of cinnamic acids and alkynes for selective construction of *E*-,*Z*-difluoroalkyl alkenes and difluoroalkyl alkenyl iodides, respectively, were achieved under mild conditions. The high efficiency, good substrate scope and high selectivity altogether highlight the prospect of Pt(II) photocatalysts in visible-light-driven organic transformation reactions.

The incorporation of a difluoromethyl (CF₂) group into organic molecules¹ to improve their physicochemical properties is particularly intriguing. Recently, visible light photo-catalysis² has emerged as a powerful tool for difluoromethylation reactions³ owing to the inherently green and mild reaction conditions. In this regard, photocatalysts play a critical role in activating substrates to generate reactive intermediates for desired transformations. Therefore, extending the diversity of photocatalysts is of significant interest. Transition metal complexes,⁴ organic dyes⁵ and heterogeneous semiconductors⁶ are commonly used photocatalysts; much attention has been focused on transition metal photocatalysts owing to their excellent photophysics and modification flexibility.

Octahedral Ru(II) and Ir(III) chromophores are common photocatalysts for organic transformations primarily *via* outer sphere interactions with substrates. Meggers and co-workers⁷ reported a type of Ir(III) complexes containing labile coordinated ligand for photochemical reactions *via* inner sphere interactions. Compared to the octahedral Ru(II) and Ir(III) chromophores, Pt(II) complexes⁸ with vacant axial coordination sites could provide greater opportunities

for both outer sphere and inner sphere interactions with substrates. However, few studies of photo-induced organic transformation reactions by Pt(II) complexes have been reported.⁹ Recently, Liu and co-workers¹⁰ reported a strategy for difluoroalkylation of cinnamic acids by harnessing the photo-redox properties of a Ru(II) complex and the reductive capability of a Cu(I) catalyst. Herein we report the high photocatalytic reactivity of Pt(II) complexes for the difluoroalkylation reactions. The present Pt(II) photo-catalysis combines photo-redox and substrate binding capabilities. Furthermore, we have extended the substrate scope of photocatalytic difluoroalkylation reactions from cinnamic acids to ethyl difluorobromoacetate and alkynes. In addition, the selectivity of *E*-,*Z*-difluoroalkyl alkenes and difluoroalkyl alkenyl iodides can be easily achieved by simply altering the reaction conditions.

A series of new cyclometalated Pt(II) complexes containing diphosphine (P^P) ligand were synthesized (Scheme 1). Details of their synthesis and characterization are given in the ESI† (Schemes S1–S3). Complex **1** was prepared by reacting Pt^{II}[R(C^N^N)]Cl (R = 4-MeOC₆H₄) with ((*R*)-(+)-2,2'-bis(diphenylphosphino)-1,1'-binaphthyl (*R*-BINAP)) in a CH₃CN/CH₃OH mixture (Scheme 1). Single-crystal X-ray analysis of **1** revealed that the Pt(II) ion is coordinated to a bidentate cyclometalating C^N ligand and a P^P



Scheme 1 Chemical structures of Pt(II) complexes and crystal structure of **1**.

^a Department of Chemistry, South University of Science and Technology of China, Shenzhen, Guangdong 518055, P. R. China. E-mail: cmche@hku.hk

^b College of Chemistry and Molecular Sciences, Wuhan University, Wuhan, Hubei 430072, P. R. China

^c State Key Laboratory of Synthetic Chemistry, Department of Chemistry, The University of Hong Kong, Pokfulam Road, Hong Kong, P. R. China

^d HKU Shenzhen Institute of Research and Innovation, Shenzhen, Guangdong 518057, P. R. China

† Electronic supplementary information (ESI) available: Experimental procedures, characterization of products, Tables S1–S3, Schemes S1–S4, and Fig. S1–S5. CCDC 1544039. For ESI and crystallographic data in CIF or other electronic format see DOI: 10.1039/c7cc03823b

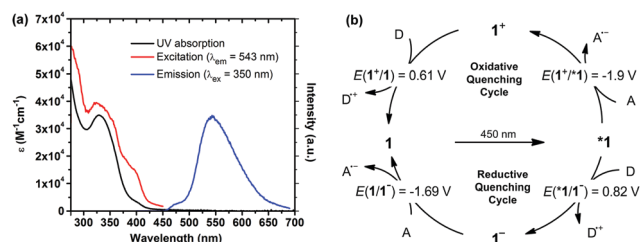


Fig. 1 (a) Electronic absorption, emission and excitation spectra of **1** (concentration ca. 1.0×10^{-5} M) in degassed CH_3CN at room temperature. (b) Excited state potential of **1**.

chelate in a distorted square planar geometry (Scheme 1) with a pending pyridyl motif.¹¹ In CH_3CN solution, **1** exhibits intense absorption at λ 300–450 nm, attributable to a mixture of metal-to-ligand and ligand-to-ligand charge transfer transitions (Fig. 1a), and a broad emission with λ 543 nm (lifetime: 93 ns, quantum yield: 0.2%) at room temperature. Nanosecond time-resolved emission (ns-TRE) and absorption (ns-TA) spectra of **1** were recorded (see the ESI,[†] Fig. S1). The ns-TA spectra are characterized by a positive signal assigned to an excited state absorption of **1** at λ 350–700 nm. The excited state potentials of **1** (Fig. 1b) can be estimated from the equations: $E(1^+/1^*) = E(1^+/1) - E_{0-0}(1)$; $E(1^*/1^-) = E(1^*/1) + E_{0-0}(1)$ ($E(1^+/1)$ and $E(1^-/1)$ were taken as the respective E_{pa} (0.61 V) and E_{pc} (−1.69 V vs. $\text{Cp}_2\text{Fe}^{+/0}$) values from the cyclic voltammogram shown in Fig. S2 (ESI[†]); E_{0-0} was estimated to be ~ 495 nm (2.51 eV).

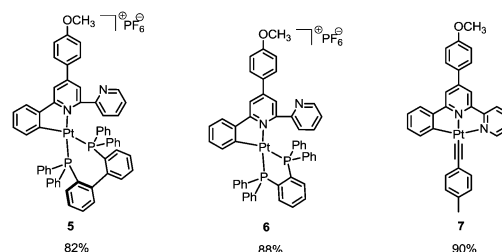
The photocatalytic activity of **1** was examined by using the coupling of cinnamic acid **a1** and ethyl difluoroiodoacetate **b1** as a model reaction. As shown in Table 1, optimization of the reaction conditions revealed that 0.5 mol% of **1** with excess sodium bicarbonate under nitrogen atmosphere resulted in highly chemo- and regio-selective generation of *E*-difluoroalkyl alkene in 90% yield. Control experiments revealed that each component of the reaction conditions was essential to the reaction efficiency. The effect of coordinated ligands on the photocatalytic activity was examined. For complexes **2**, **3**, and **4** having no methoxyl

Table 1 Optimization of reaction conditions^a

Entry	Conditions ^a	Yield of c1 ^b (%)
1	1% 1 , CH_3CN , N_2	—
2	1% 1 , 1.1 equiv. NaHCO_3 , CH_3CN , N_2	92
3	0.5% 1 , 1.1 equiv. NaHCO_3 , CH_3CN , N_2	90
4	0.5% 1 , 1.1 equiv. NaHCO_3 , CH_3CN , air	—
5	1.1 equiv. NaHCO_3 , CH_3CN , N_2	—
6	0.5% 2 , 1.1 equiv. NaHCO_3 , CH_3CN , N_2	25
7	0.5% 3 , 1.1 equiv. NaHCO_3 , CH_3CN , N_2	65
8	0.5% 4 , 1.1 equiv. NaHCO_3 , CH_3CN , N_2	42
9	2% $\text{Ru}(\text{bpy})_3\text{Cl}_2$, 1.1 equiv. NaHCO_3 , CH_3CN , N_2	Trace
10	2% $\text{Ir}[(\text{dtbpy})(\text{ppy})_2]\text{PF}_6$, 1.1 equiv. NaHCO_3 , CH_3CN , N_2	30
11	2% $\text{Ir}(\text{ppy})_3$, 1.1 equiv. NaHCO_3 , CH_2Cl_2 , N_2	45

^a 0.2 mmol **a1**, 0.22 mmol **b1**, 5 mL solvent, blue LED irradiation.

^b Isolated yield.



Scheme 2 Other efficient Pt(II) photocatalysts for difluoroalkylation reactions.

benzyl group or no pending pyridyl motif in the bidentate C^*N ligand scaffold, moderate reactivity was observed (Table 1, entries 6–8). However, similar good reactivity was observed when the diphosphine ligand was changed to 2,2'-bis(diphenylphosphino)-1,1'-biphenyl (**5**) or 1,2-bis(diphenylphosphino)benzene (**6**) (Scheme 2). The other Pt(II) complex $\text{Pt}^{\text{II}}[\text{R}(\text{C}^*\text{N}^*)][\text{CCC}_6\text{H}_4\text{-4-Me}]$ ($\text{R} = 4\text{-MeOC}_6\text{H}_4$, **7**)¹² was also found to be good photocatalyst for this reaction. Furthermore, $\text{Ir}[(\text{dtbpy})(\text{ppy})_2]\text{PF}_6$ and $\text{Ir}(\text{ppy})_3$ were also observed to exhibit photo-activity for this reaction with moderate product yields (30%, 45%), while $\text{Ru}(\text{bpy})_3\text{Cl}_2$ gave trace amount of **c1** (Table 1, entries 9–11). We conceive that the excited state reduction potential of $\text{Ru}(\text{bpy})_3\text{Cl}_2$ is not sufficient to reduce **b1** to generate reactive intermediate, and inner-sphere substrate binding may facilitate the Pt(II) photo-catalysis. Notably, for substrate **a1**, the reaction proceeded smoothly on a gram scale with a 72% product yield (Table 2, **c1**).

As shown in Table 2, a wide range of cinnamic acids were readily converted to their corresponding *E*-difluoroalkenes in good to excellent yields. Both electron-withdrawing and -donating substituents on the aromatic ring of the cinnamic acids were well tolerated (Table 2, **c1**–**c24**). Notably, upon substitution of the α,β -vinyl carboxylic acids at the β -position, no obvious decrease in the reaction efficiency was observed (Table 2, **c25**, **c26**). However, when the α -position was occupied by a methyl group (Table 2, **c27**), the product yield decreased sharply to 30% attributed to steric hindrance. Unfortunately, alkyl-substituted α,β -vinyl carboxylic acid

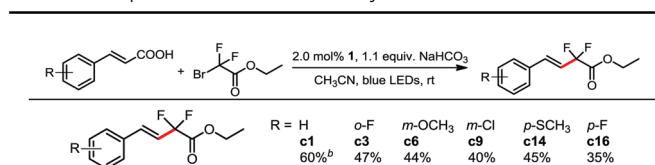
Table 2 Scope of cinnamic acids^a

R	H	O-CH_3	O-F	O-Cl	O-Br	m-O-CH_3	m-CH_3	m-F	m-Cl	m-Br
c1	90% ^b	c2	c3	c4	c5	c6	c7	c8	c9	c10
(1.63 g, 72%)										
R = p-CH_3	c11	$\text{p-CO}_2\text{CH}_3$	p-OCH_3	p-SCH_3	p-CHO	p-F	p-Cl	p-CN	p-NO_2	
	87%	72%	83%	89%	63%	84%	75%	86%	78%	

c20 , 88%	c21 , 82%	c22 , 83%
c23 , 82%	c24 , 53%	c25 , 92%
c26 , 75%	c27 , 30%	c28 , 0% ^c

^a 0.2 mmol **a**, 0.22 mmol **b**, 0.5 mol% **1** and 1.1 equiv. NaHCO_3 were dissolved and degassed for 15 min, blue LED irradiation for 12 h.

^b Isolated yield. ^c Starting materials recovered.

Table 3 Scope of cinnamic acids in ethyl difluorobromoacetate reaction^a

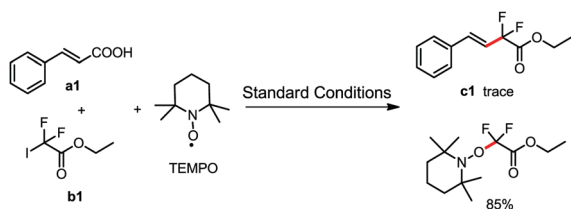
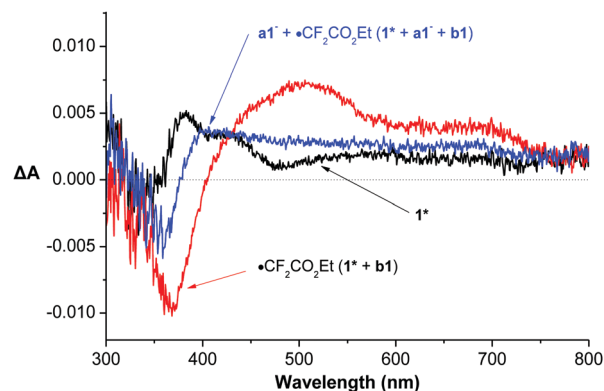
^a 0.2 mmol **a**, 0.6 mmol **b2**, 2 mol% **1** and 1.1 equiv. NaHCO₃ were dissolved and degassed for 15 min, blue LED irradiation for 12 h.

^b Isolated yield.

(Table 2, **c28**) was ineffective in this catalytic system. Further experiments showed that this reaction could be extended to ethyl difluorobromoacetate with moderate product yields (Table 3).

In subsequent mechanistic investigation, we found that a radical inhibitor (2,2,6,6-tetramethyl-1-piperidinyloxy (TEMPO)) completely inhibited the reaction and afforded the TEMPO-trapped difluoroacetyl product in 85% yield, revealing that a difluoroacetyl radical was involved in the reaction (Scheme 3). When **1** was mixed with substrate **b1**, a species with a molecular weight of [**1** + HI] was detected by high-resolution mass spectrometry (HRMS) (Fig. S3, ESI[†]). This result, along with the emission quenching of **1** by **b1** (Fig. S4, ESI[†]), suggests that inner sphere interaction occurred between **b1** and **1**. Furthermore, the oxidation potential of the excited state of **1** ($E(1^+/1^*)$) was estimated to be -1.90 V vs. Cp₂Fe⁺⁰. The E_{pc} of substrate **b1** was measured to be -1.66 V vs. Cp₂Fe⁺⁰ by cyclic voltammetry, as shown in Fig. S5 (ESI[†]). Therefore, the free energy change (ΔG) was estimated to be -0.24 eV using the equation: $\Delta G = E_{ox} - E_{red} - E_{00}$. Therefore, the photoinduced electron transfer from **1** to **b1** is thermodynamically feasible.

The ns-TA spectra of **1**, recorded immediately after the laser flash and in the absence of **a1**, presence of **a1** and presence of deprotonated **a1** (noted as **a1**[−]), are similar (Fig. S4a, ESI[†]), with a positive absorption band at 350–500 nm region. Remarkably, the ns-TA spectrum of **1** in the presence of **b1** (Fig. 2) exhibited a distinctive spectral profile with a negative bleaching signal at 363 nm and a broad positive band at wavelength beyond 410 nm. Kinetic analysis of the decay at 363 nm revealed a species that was stable beyond 300 μs with a decay time constant of around 130 μs (Fig. S4, ESI[†]). This long-lived species, which is assigned to the difluoroacetyl radical ([•]R_F), could be further quenched by **a1**[−], leading to new species with a different time-resolved absorption spectral profile and a peak maximum at 400 nm. Kinetic studies of this peak yielded one short-lived growth component and one long-lived decay component with time constants of 4.2 μs and 158 μs, respectively

**Scheme 3** The radical inhibitor TEMPO inhibited the reaction.**Fig. 2** ns-TA spectra of **1** (5×10^{-5} M) in CH₃CN in the presence of 20 equiv. of substrate **b1** and **a1**[−] + **b1** (1 mM for each component) after 355 nm laser excitation recorded at 0 s.

(Fig. S4h, ESI[†]). This short-lived component is attributed to the reaction between **a1**[−] with [•]R_F, and the long-lived component is assigned to a radical species of the product (**s-1** in Scheme 4).

Based on these results, a plausible reaction pathway is proposed (Scheme 4). Upon excitation of **1** by visible light, a single electron-transfer reduction of R_FI by excited Pt(II) complex **1**^{*} generates one-electron-oxidized species **1**⁺ and radical [•]R_F, and the latter reacts with the deprotonated α,β-vinyl carboxylic acids **a**[−] to generate radical **s-1**. Subsequent oxidation of **s-1** by **1**⁺ generated carboxyl radical intermediate **s-2**, which gave the desired *E*-difluoroacetyl alkene **c** through a decarboxylation process. The role of the carboxylic acid group on the alkenes was revealed using styrene having no COOH group as the substrate (Scheme S4, ESI[†]). In this case, only a 25% product yield was obtained, suggesting that both the deprotonated carboxylic acid and substrate play a vital role in the recovery of photocatalyst **1**.

As depicted in Scheme 4, the difluoroacetyl radical could be efficiently generated by the Pt(II) photocatalyst. We speculate that this radical intermediate may be able to perform more reactions. Indeed, when terminal aryl alkyne was added to CH₃CN solution containing 0.5 mol% **1** and 1.1 equivalent of **b1**, the difluoroacetyl alkenyl iodide product was formed in good to excellent yields with good selectivity irrespective of the substituent(s) on the aryl group (Table 4). In addition, *E*-difluoroacetyl alkenyl iodides were the major products. When the *ortho*-position of the terminal aryl alkyne was substituted, the products were formed with good selectivity (Table 4, **c41–c45**). A plausible reaction pathway is

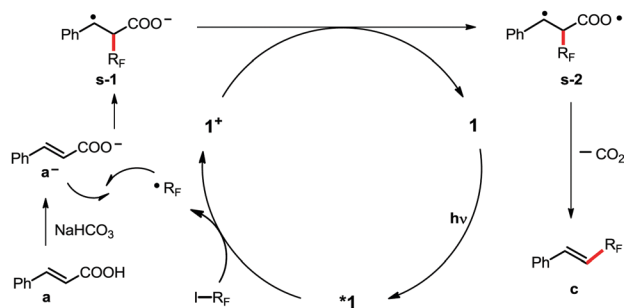
**Scheme 4** Proposed reaction pathway.

Table 4 Alkyne scope in atom transfer radical addition reactions^a

R ¹	c	Yield (%)	E/Z	R ¹	c	Yield (%)	E/Z
p-H	c29	93% ^b	6:1	p-CN	c35	61%	25:1
p-OCH ₃	c30	96%	3:1	p-F	c36	85%	6:1
p-CH ₃	c31	83%	6:1	p-CO ₂ Et	c37	72%	6:1
p-Cl	c32	82%	6:1	p-NO ₂	c38	70%	20:1
p-Br	c33	75%	6:1	m-OCH ₃	c39	92%	6:1
p-CF ₃	c34	81%	6:1	m-Br	c40	85%	6:1

R ²	c	Yield (%)	E/Z
CH ₃	c41	78%	20:1
OCH ₃	c42	68%	30:1
CHO	c43	75%	15:1
Cl	c44	80%	25:1
Br	c45	80%	25:1

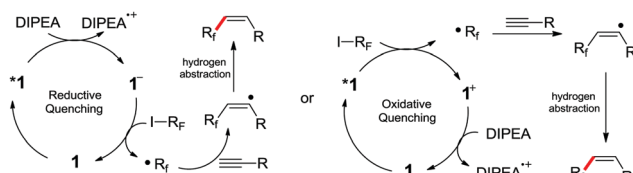
^a 0.2 mmol alkynes, 0.22 mmol **b1**, 0.5 mol% **1** were dissolved and degassed for 15 min, blue LED irradiation for 6 h. ^b Isolated yield.

Table 5 Alkyne scope in Z-difluoroalkyl alkene generation reactions^a

R	c	Yield (%)	Z/E	R	c	Yield (%)	Z/E
H	c46	82% ^b	10:1	p-CH ₃	c47	81%	10:1
p-CH ₃	c47	81%	10:1	p-Cl	c48	71%	10:1
p-Cl	c48	71%	10:1	p-Br	c49	73%	10:1
p-Br	c49	73%	10:1	m-CH ₃	c50	75%	10:1
m-CH ₃	c50	75%	10:1	o-CH ₃	c51	78%	15:1
o-CH ₃	c51	78%	15:1	o-OCH ₃	c52	74%	25:1
o-OCH ₃	c52	74%	25:1	o-Cl	c53	76%	30:1
o-Cl	c53	76%	30:1	o-Br	c54	73%	20:1

R	c	Yield (%)	Z/E	R	c	Yield (%)	Z/E
H	c55	72%	10:1	p-CH ₃	c56	63%	10:1
p-CH ₃	c56	63%	10:1	p-Cl	c57	53%	10:1
p-Cl	c57	53%	10:1	p-Br	c58	58%	10:1
p-Br	c58	58%	10:1	m-CH ₃	c59	55%	10:1
m-CH ₃	c59	55%	10:1	o-CH ₃	c60	59%	20:1
o-CH ₃	c60	59%	20:1	o-OCH ₃	c61	57%	Z only
o-OCH ₃	c61	57%	Z only	o-Cl	c62	60%	Z only
o-Cl	c62	60%	Z only	o-Br	c63	61%	Z only

^a 0.2 mmol alkynes, 0.22 mmol **b1**, 0.5 mol% **1**, 5.0 equiv. DIPEA were dissolved and degassed for 15 min, blue LED irradiation for 12 h. ^b Isolated yield.



Scheme 5 Proposed reaction pathway.

shown in Scheme S5 (ESI[†]). Photoreduction of **b1** by **1** generated one-electron oxidized species **1**⁺ and difluoroacetyl radical (**R_F**[•]). The **R_F**[•] radical reacts with the terminal alkyne to afford difluoroacetyl alkenyl radical **s-3**, the latter abstracts an iodine atom from **b1** to generate the final product.

When an organic base such as *N,N*-diisopropylethylamine (DIPEA) was added to the reaction mixture, *Z*-difluoroalkyl alkenes rather than difluoroacetyl alkenyl iodides were obtained in good yields (Table 5). When methanol was present in the reaction mixture, an interesterification phenomenon was observed with methyl difluoroacetyl alkenes observed in good selectivity and moderate yields. The strong basicity of DIPEA is most likely responsible for the inter-esterification process. When the *ortho*-position of the terminal aryl alkyne was substituted, the selectivity was moderately good (Table 5, **c51–c54** and **c60–c63**). As shown in Scheme 5, DIPEA acted as an electron donor as well as a hydrogen donor.

In summary, the Pt(II) photo-catalyzed controlled and selective difluoroalkylation reactions of cinnamic acids and alkynes affording *E*-*Z*-difluoroalkyl alkenes and difluoroalkyl alkenyl iodides, respectively, have been reported. The high efficiency, good substrate scope and high selectivity highlight the promise of Pt(II) photo-catalysis in visible-light-driven organic transformation reactions.

This work was supported by the National Natural Science Foundation of China (21272197), National Key Basic Research Program of China (973 Program 2013CB834802), and Science and Technology Innovation Commission of Shenzhen Municipality (JCYJ20160229123546997).

Notes and references

- (a) D. O'Hagan, *Chem. Soc. Rev.*, 2008, **37**, 308–319; (b) S. Purser, P. R. Moore, S. Swallow and V. Gouverneur, *Chem. Soc. Rev.*, 2008, **37**, 320–330.
- (a) D. A. Nicewicz and D. W. C. MacMillan, *Science*, 2008, **322**, 77–80; (b) K. Zeitler, *Angew. Chem., Int. Ed.*, 2009, **48**, 9785–9789; (c) T. P. Yoon, M. A. Ischay and J. Du, *Nat. Chem.*, 2010, **2**, 527–532; (d) J. M. R. Narayanan and C. R. J. Stephenson, *Chem. Soc. Rev.*, 2011, **40**, 102–113; (e) M. Rueping, D. Leonori and T. Poisson, *Chem. Commun.*, 2011, **47**, 9615–9617; (f) J. Xuan and W.-J. Xiao, *Angew. Chem., Int. Ed.*, 2012, **51**, 6828–6838.
- (a) Q. Lin, L. Chu and F.-L. Qing, *Chin. J. Chem.*, 2013, **31**, 885–891; (b) Y.-M. Su, Y. Hou, F. Yin, Y.-M. Xu, Y. Li, X. Zheng and X.-S. Wang, *Org. Lett.*, 2014, **16**, 2958–2961; (c) N. Iqbal, J. Jung, S. Park and E. J. Cho, *Angew. Chem., Int. Ed.*, 2014, **53**, 539–542; (d) P. Xu, G. Wang, Y. Zhu, W. Li, Y. Cheng, S. Li and C. Zhu, *Angew. Chem., Int. Ed.*, 2016, **55**, 2939–2943; (e) J. Xie, T. Zhang, F. Chen, N. Mehrkens, F. Rominger, M. Rudolph and A. S. K. Hashmi, *Angew. Chem., Int. Ed.*, 2016, **55**, 2934–2938.
- (a) W.-P. To, G. S.-M. Tong, W. Lu, C. Ma, J. Liu, A. L.-F. Chow and C.-M. Che, *Angew. Chem., Int. Ed.*, 2012, **51**, 2654–2657; (b) C. K. Prier, D. A. Rankic and D. W. C. MacMillan, *Chem. Rev.*, 2013, **113**, 5322–5363; (c) G. Revol, T. McCallum, M. Morin, F. Gagosz and L. Barriault, *Angew. Chem., Int. Ed.*, 2013, **52**, 13342–13345.
- (a) D. P. Hari and B. König, *Org. Lett.*, 2011, **13**, 3852–3855; (b) Q. Liu, Y.-N. Li, H.-H. Zhang, B. Chen, C.-H. Tung and L.-Z. Wu, *Chem. – Eur. J.*, 2012, **18**, 620–627; (c) N. A. Romero and D. A. Nicewicz, *Chem. Rev.*, 2016, **116**, 10075–10166.
- (a) F. Su, S. C. Mathew, L. Möhlmann, M. Antonietti, X. Wang and S. Blechert, *Angew. Chem., Int. Ed.*, 2011, **50**, 657–660; (b) X.-B. Li, Z.-J. Li, Y.-J. Gao, Q.-Y. Meng, S. Yu, R. G. Weiss, C.-H. Tung and L.-Z. Wu, *Angew. Chem., Int. Ed.*, 2014, **53**, 2085–2089.
- H. Huo, X. Shen, C. Wang, L. Zhang, P. Röse, L.-A. Chen, K. Harms, M. Marsch, G. Hilt and E. Meggers, *Nature*, 2014, **515**, 100–103.
- (a) D. M. Roundhill, H. B. Gray and C.-M. Che, *Acc. Chem. Res.*, 1989, **22**, 55–61; (b) R. McGuire Jr., M. C. McGuire and D. R. McMillin, *Coord. Chem. Rev.*, 2010, **254**, 2574–2583.
- (a) J.-J. Zhong, Q.-Y. Meng, G.-X. Wang, Q. Liu, B. Chen, K. Feng, C.-H. Tung and L.-Z. Wu, *Chem. – Eur. J.*, 2013, **19**, 6443–6450; (b) W. J. Choi, S. Choi, K. Ohkubo, S. Fukuzumi, E. J. Cho and Y. You, *Chem. Sci.*, 2015, **6**, 1454–1464; (c) D. P. Shelar, T.-T. Li, Y. Chen and W.-F. Fu, *Chem-PlusChem*, 2015, **80**, 1541–1546; (d) P.-K. Chow, G. Cheng, G. S. M. Tong, W.-P. To, W.-L. Kwong, K.-H. Low, C.-C. Kwok, C. Ma and C.-M. Che, *Angew. Chem., Int. Ed.*, 2015, **54**, 2084–2089; (e) F. Juliá and P. González-Herrero, *J. Am. Chem. Soc.*, 2016, **138**, 5276–5282.
- H.-R. Zhang, D.-Q. Chen, Y.-P. Han, Y.-F. Qiu, D.-P. Jin and X.-Y. Liu, *Chem. Commun.*, 2016, **52**, 11827–11830.
- W. Lu, M. C. W. Chan, N. Zhu, C.-M. Che, C. Li and Z. Hui, *J. Am. Chem. Soc.*, 2004, **126**, 7639–7651.
- W. Lu, B.-X. Mi, M. C. W. Chan, Z. Hui, C.-M. Che, N. Zhu and S.-T. Lee, *J. Am. Chem. Soc.*, 2004, **126**, 4958–4971.